MOLECULAR AND CELLULAR BIOLOGY, Nov. 2009, p. 5800–5812 Vol. 29, No. 21
0270-7306/09/$12.00 doi:10.1128/MCB.00684-09
Copyright © 2009, American Society for Microbiology. All Rights Reserved.

Regulation of Myoblast Differentiation by the Nuclear Envelope Protein NET39▽†

Guang-Hui Liu, Tinglu Guan, Kaustuv Datta, Judith Coppinger, John Yates III, and Larry Gerace*

Department of Cell Biology, Scripps Research Institute, La Jolla, California 92037

Received 26 May 2009/Returned for modification 5 July 2009/Accepted 11 August 2009

Recently, several transmembrane proteins of the nuclear envelope have been implicated in regulation of signaling and gene expression. Here we demonstrate that the nuclear lamina-associated *n*uclear *e*nvelope *t*ransmembrane protein NET39 (Ppapdc3) functions as a negative regulator of myoblast differentiation, in part through effects on mTOR signaling. We found that NET39 is highly expressed in cardiac and skeletal muscle tissues and becomes strongly upregulated during cultured myoblast differentiation. Knockdown of NET39 by RNA interference in myoblasts strongly promoted differentiation, whereas overexpression of NET39 repressed myogenesis. Proteomic analysis of NET39 complexes immunoprecipitated from myotubes, in combination with other methods, identified mTOR as an interaction partner of NET39. We found that ectopic expression of NET39 in myoblasts negatively regulated myogenesis by diminishing mTOR activity, which in turn decreased insulin-like growth factor II production and autocrine signaling. Our results indicate that NET39 is part of the regulatory machinery for myogenesis and raise the possibility that it may be important for muscle homeostasis.

The nuclear envelope (NE) forms a selective barrier that separates the cytoplasm from the nuclear interior in eukaryotes. The NE contains an inner nuclear membrane (INM) and an outer nuclear membrane that are joined at nuclear pore complexes, large supramolecular assemblies that provide transport channels across the NE. The INM is lined by the nuclear lamina, a protein meshwork containing a polymer of the lamin intermediate filament proteins and numerous more minor components, including transmembrane proteins of the INM. Lamins and associated transmembrane proteins provide a scaffold for organizing chromatin and nuclear structure. In addition, it has become clear that lamina components also regulate signaling and gene expression (8, 21, 41). Recent work has implicated the INM proteins emerin and MAN1 in regulation of signaling. MAN1 has been found to bind directly to R-Smad proteins and, as a consequence, to attenuate transforming growth factor beta and BMP signaling (2). Emerin has been implicated in the Rb1/E2F and MyoD pathways of gene expression during muscle regeneration (16, 29), and its loss causes hyperactivation of mitogen-activated protein kinase pathways in the heart and myoblasts (30). The finding that mutations in lamina-associated proteins lead to numerous human diseases ("laminopathies") can be explained, at least in part, by the signaling-related functions of these proteins.

Our laboratory identified over 50 novel putative NE-specific transmembrane proteins (NETs) from a proteomic analysis, substantially increasing the list of ~15 integral proteins of the NE that had been identified at that time (38). Expression profiling showed that six of the NETs are significantly upregulated at the transcriptional level during myoblast differentiation. The most strongly upregulated of this group, NET39 (Ppapdc3), contains a lipid phosphate phosphatase (LPP) homology domain (6). This suggests a potential role of NET39 in signaling. However, until now nothing is known about its biological functions and its potential relationship to myogenic differentiation.

Skeletal muscle development involves a highly ordered cascade of events comprising myogenic lineage commitment, myoblast proliferation, and terminal differentiation. Myogenesis critically depends on a group of basic helix-loop-helix (bHLH) transcription factors. The bHLH proteins Myf5 and MyoD are expressed prior to differentiation and specify commitment to the myoblast lineage. Conversely, the bHLH proteins MRF4 and myogenin are expressed only after myoblast withdrawal from the cell cycle and drive the decisive events of myogenic differentiation, including myoblast fusion and the expression of characteristic muscle proteins, such as skeletal muscle myosin heavy chain (MyHC) (5).

Coordination of myoblast differentiation is achieved through endocrine and paracrine/autocrine effects on several signaling pathways, which activate the expression of myogenin, MRF4, and other late myogenic genes (33, 47). The insulin-like growth factors (IGFs), including IGF-I and IGF-II, play critical roles in skeletal muscle differentiation and growth as well as in adult muscle regeneration and hypertrophy (13, 31, 32). In myoblast culture, the autocrine/paracrine actions of IGF-II, induced in response to growth factor deprivation, are instrumental in myogenic differentiation (11, 14, 36, 44). The transcriptional induction of IGF-II after experimental induction of myoblast differentiation is controlled by the Ser/Thr kinase mammalian target of rapamycin (mTOR) (11, 49, 50). Although mTOR is required for IGF-II expression, the kinase activity of mTOR appears to be dispensable for this process (10, 11, 35). To date, little is known about how the mTOR–IGF-II axis is regulated during myogenesis.

Here we characterize the properties of NET39 and describe its effects on myogenesis in C2C12 myoblasts. Using gene si-

* Corresponding author. Mailing address: Department of Cell Biology, IMM-10, Scripps Research Institute, 10550 North Torrey Pines Road, La Jolla, CA 92037. Phone: (858) 784-8514. Fax: (858) 784-0132. E-mail: lgerace@scripps.edu.

† Supplemental material for this article may be found at http://mcb.asm.org/.

▽ Published ahead of print on 24 August 2009.

lencing and ectopic overexpression approaches, we find that the presence of NET39 in myoblasts negatively regulates myogenic differentiation. This inhibitory phenotype is explained by our finding that NET39 interacts with mTOR and that it represses mTOR-mediated IGF-II secretion. We propose that NET39, which is induced to high levels following myogenic differentiation, functions in muscle homeostasis by limiting the expression of myogenic genes. We also suggest that regulation of NET39 may be important in muscle regeneration and hypertrophy.

MATERIALS AND METHODS

Reagents and antibodies. Phosphatidic acid (PA; C_8), lysophosphatidic acid (LPA; $C_{18:1}$), and diacylglycerol pyrophosphate (DGPP; C_8) were purchased from Avanti Polar Lipids. Ceramide-1-phosphate (C1P), sphingosine-1-phosphate (S1P), polyisoprenyl phosphate, farnesyl diphosphate (FDP), rapamycin, 1-butanol, and IGF-II were purchased from Sigma. R59022 (diacylglycerol kinase inhibitor I) was purchased from Calbiochem. To construct NET39-V5, NET39(1-100)-V5, NET39(72-271)-V5, NET39(92-271)-V5, and LPP3-V5, corresponding cDNA fragments were PCR amplified from NET39 or LPP3 cDNA clones (Open Biosystems) and ligated into the pcDNA 3.1 D/V5-His-TOPO vector (Invitrogen). Myc-NET39 was generated by subcloning NET39 cDNA into the BamHI and XhoI sites of the Dual-CCM(N-Myc) vector (Vector Biolabs). All of the clones were confirmed by DNA sequencing. Myc-mTOR and its truncation mutants were kindly provided by Do-Hyung Kim (45), and H19-luc-ME was a generous gift of Jie Chen (11). SureSilencing short hairpin RNA (shRNA) plasmids for mouse Ppapdc3/NET39 with a U1 promoter and neomycin resistance gene were obtained from SABiosciences. The sense sequences were as follows: shCtrl, GGAATCTCATTCGATGCATAC; shNET39#2, TAC CTCACCATGGACATCTAT; shNET39#3, AGCCCTGCTCTTGGACAT CAT; and shNET39#4, ATCGGACGCCACCACATTACA. Purified adenovirus encoding MyoD or carrying an empty cytomegalovirus cassette was purchased from Vector Biolabs. Adenovirus encoding Myc-NET39 (Ad-Myc-NET39) was generated by using Dual-CCM (N-Myc)-NET39 as a shuttle vector. Construction and purification of Ad-Myc-NET39 were carried out by Vector Biolabs. Anti-NET39 polyclonal antibody was generated in rabbits, using a recombinant His-tagged protein comprising the N-terminal 105 amino acids of murine NET39, and was affinity purified against the latter. The following antibodies were obtained commercially: anti-Myc (Santa Cruz Biotechnology, Inc.), anti-V5 (Invitrogen), anti-PDI (Stressgen), antimyogenin (BD Pharmingen), anti-MyHC (U.S. Biological), anti-alpha-tubulin and anti-H2B (Abcam), anti-calnexin (BD Transduction Laboratories), anti-mTOR (Cell Signaling Technology and Santa Cruz Biotechnology, Inc.), anti-phospho-p70S6K (Cell Signaling Technology), anti-IGF-II (R&D Systems), anti-V5 and anti-Myc agarose (Sigma), Alexa Fluor488- or Alexa Fluor594-conjugated anti-immunoglobulin G (anti-IgG) antibody (Invitrogen), and horseradish peroxidase-conjugated anti-IgG antibodies (Pierce).

Cell culture and transfection. HEK293A cells (Invitrogen), HeLa cells (ATCC), COS-7 cells (ATCC), and CH3-10T1/2 cells (ATCC) were maintained in Dulbecco's modified Eagle's medium (DMEM) supplemented with 10% fetal bovine serum (FBS) (Invitrogen) and antibiotics. C2C12 cells (ATCC) were maintained in proliferation medium (PM; DMEM supplemented with 15% FBS and antibiotics). For differentiation assays, cells were seeded in 12-well cell culture plates (Corning Incorporated) in PM at 50% confluence, grown to confluence, and then switched to differentiation medium (DM; same as PM, but with 2% horse serum [HS; Invitrogen] instead of FBS). This time point was considered day 0 of differentiation (DM0). The DM was replaced every day. For HeLa, HEK293A, and COS-7 cells, cells were transfected with Lipofectamine 2000 (Invitrogen) according to the manufacturer's instructions. For C2C12 cells, DNA transfections were performed in 12-well plates with 2×10^5 cells suspended in 1 ml PM, using 1 μg plasmid DNA and 10 μl Optifect (Invitrogen) per reaction. Stable C2C12 populations containing various shRNA expression constructs were generated by selection with 1,000 μg/ml G418 for 1 week, followed by 500 μg/ml G418 for 2 weeks.

Gene transfer with recombinant adenoviruses. Before infection, purified adenoviruses (Ad-empty or Ad-Myc-NET39) were diluted in DMEM with 2% FBS (for C2C12 myoblasts) or with 2% HS (for C2C12 myotubes) and filtered through a 0.45-μm syringe filter (Gelman). Viruses were added to cells at 37°C for 8 h, to a final concentration of 2×10^8 inclusion-forming units (IFU)/ml. Cells were then washed twice with phosphate-buffered saline (PBS) and incubated with the growth medium (for myoblasts) or with DM (for myotubes) for specific purposes. Under these conditions, nearly 100% of cells were infected with viruses, as evaluated by immunofluorescence staining with anti-Myc antibody.

Immunofluorescence microscopy. Cells were fixed with 4% formaldehyde in PBS for 10 min at room temperature (RT), either with or without preextraction with Triton X-100 before fixation. For Triton preextraction, cells were rinsed once with PBS and then extracted twice with 1% Triton X-100 in 10 mM Tris-HCl, pH 7.5, 1.5 mM $MgCl_2$, and 2 mM $CaCl_2$ for 30 s at RT. Following fixation, cells were treated with 0.2% Triton X-100 in PBS for 5 min at RT or with 30 μg/ml digitonin in 0.3 M sucrose, 1.5 mM $MgCl_2$, 120 mM KCl, 0.15 mM $CaCl_2$, 2 mM EGTA, and 25 mM HEPES-KOH (pH 7.6) for 10 min on ice. After being blocked with 10% FBS in PBS for 20 min, cells were incubated for 1 h with primary antibody, followed by washing in PBS and incubation for 1 h with the relevant secondary antibody. Nuclei were stained with Hoechst 33342 (Invitrogen). The stained cells on coverslips were subsequently mounted in Gel Mount (Biomeda) and sealed with Clarion mounting medium (Biomeda). Cell images were taken with a Bio-Rad–Zeiss Radiance 2100 laser scanning confocal microscope and analyzed by LaserSharp 2000 software (Bio-Rad). Images were pseudocolorized and merged with ImageJ. For MyHC immunostaining, images were acquired on a Leica DM IRE2 microscope equipped with a Hamamatsu C4742-95 digital charge-coupled device camera. Images were analyzed using ImageJ to determine the percentage of nuclei within MyHC-positive areas.

Immunoprecipitation and immunoblotting. For immunoprecipitation studies, whole-cell extracts were prepared by scraping cells into ice-cold lysis buffer (50 mM Tris, pH 7.5, 250 mM NaCl, 1 mM EDTA, 1 mM EGTA, 0.5% Triton X-100, 10% glycerol, Complete protease inhibitor cocktail [Roche Diagnostics]). Samples were sonicated on ice and immunoprecipitated by incubating with anti-V5 or anti-Myc agarose or anti-NET39 antibody followed by protein A/G Plus (Santa Cruz Biotechnology, Inc.). Precipitated proteins were washed five times in lysis buffer, dissolved in sodium dodecyl sulfate sample buffer, electrophoresed in 4 to 20% Tris-glycine-sodium dodecyl sulfate gels (Invitrogen), and transferred onto nitrocellulose membranes. Membranes were probed with specific primary and horseradish peroxidase-coupled secondary antibodies at appropriate dilutions and developed with SuperSignal West Pico reagent (Pierce).

Lipid phosphatase activity analysis. Five 10-cm plates of HEK293A cells were transfected with pcDNA3, NET39-V5, or LPP3-V5, and 48 h later, cells were lysed by being scraped into ice-cold lysis buffer (50 mM Tris, pH 7.5, 250 mM NaCl, 1 mM EDTA, 1 mM EGTA, 0.5% Triton X-100, 10% glycerol, Complete protease inhibitor cocktail [Roche Diagnostics]). Samples were sonicated on ice and centrifuged at 16,000 × *g* at 4°C for 30 min. The supernatant was mixed with anti-V5 agarose and rotated at 4°C overnight. The beads were washed with lysis buffer four times and with assay buffer (100 mM Tris-maleate, pH 6.5, 0.5% Triton X-100, 10 mM dithiothreitol) twice. The recombinant NET39-V5 or LPP3-V5 protein was eluted by incubation with 70 μl V5 peptide (100 μg/ml) in assay buffer for 1 h at 4°C with agitation. After brief centrifugation, the supernatants were analyzed either by immunoblotting with anti-V5 antibody or by analysis of LPP activity by the malachite green colorimetric assay as described previously (17, 43), with minor modifications. In brief, the assays were performed in 96-well, clear, nonbinding surface assay plates (Corning Incorporated) in 40 μl of assay buffer containing either PA, LPA, C1P, S1P, DGPP, or FDP at 100 μM in the absence or presence of 10 μl of immunopurified NET39-V5 or LPP3-V5. The reaction was carried out at 37°C for 90 min and stopped with 100 μl of malachite green reagent (Biomol), and the absorbance was read at 650 nm according to the manufacturer's instructions. The enzyme reactions were linear over time and protein concentration.

Nucleus and ER membrane isolation. C2C12 cells grown in four 10-cm dishes were induced to differentiate for 4 days. Differentiated cultures were placed on ice and washed twice with ice-cold PBS, followed by once with HB (10 mM HEPES, 10 mM KCl, 1.5 mM $MgCl_2$). The cells were then scraped into a total of 1 ml HB and allowed to swell on ice for 15 min. Next, cells were Dounce homogenized with 15 strokes and mixed with 2.4 M sucrose in HB to bring the final sucrose concentration to 1.8 M. The sample was then placed in a Beckman SW41 centrifuge tube and overlaid with 3 ml 1.6 M sucrose in HB and then with 1 ml HB. After spinning at 150,000 × *g* at 4°C for 4 h in a Beckman SW41 rotor, 500 μl of each fraction, from top to bottom, was carefully removed, and an aliquot of each fraction was observed under a light microscope. The interface between the 1.6 M and 1.8 M sucrose layers contained a mixture of membrane aggregates and nuclei. The lowest 500 μl of the 1.8 M sucrose fraction contained only nuclei and no membrane debris and was used as the nuclear fraction. The interface between the HB and 1.6 M sucrose layers contained only membranes and no nuclei and was chosen as the microsomal membrane (endoplasmic retic-

ulum [ER]) fraction. Finally, the nuclear and ER fractions were subjected to immunoblotting with appropriate antibodies.

MudPIT analysis of NET39-associated proteins in myotubes. Six 10-cm plates of C2C12 myotubes (DM4) were transduced with Myc-NET39 or control adenovirus and maintained in culture for another 2 days. Cells then were washed twice with PBS and lysed in a total of 6 ml ice-cold buffer B (50 mM Tris, pH 7.5, 250 mM NaCl, 1 mM EDTA, 1 mM EGTA, 0.5% Triton X-100, 10% glycerol, Complete protease inhibitor cocktail [Roche Diagnostics]). The Myc-NET39 and control samples were immunoadsorbed to 100 μl of anti-Myc agarose by rotation at 4°C overnight. Both the control and Myc-NET39 immunoprecipitates were washed six times with buffer B and twice with PBS. The protein complexes were eluted by two sequential incubations with 8 M urea at RT for 30 min, with agitation. The supernatants of the two samples were subjected to multidimensional protein identification technology (MudPIT) analysis (46, 48). The MudPIT experiment was performed as follows. Peptides were pressure loaded onto a 100-μm-internal-diameter fused silica capillary column packed with a 5-cm-long 5-μm Partisphere strong cation exchanger (SCX) and a 5 cm of 5-μm Gemini C_{18} material (Phenomenex), with the SCX end fritted with immobilized Kasil 1624 (PQ Corporation). After being desalted, a 100-μm-internal-diameter capillary with a 5-μm pulled tip packed with 15 cm of 5-μm Jupiter C_{18} material was attached to the SCX end with a ZDV union, and the entire column was placed inline with an Agilent pump (Agilent Technologies) and analyzed using a four-step separation. The three buffer solutions used were 5% acetonitrile–0.1% formic acid (buffer A), 80% acetonitrile–0.1% formic acid (buffer B), and 500 mM ammonium acetate–5% acetonitrile–0.1% formic acid (buffer C). The first step consisted of a 100-min gradient from 0 to 100% buffer B. Steps 2 and 3 had the following profile: 3 min of 100% buffer A, 5 min of *X*% buffer C, a 10-min gradient from 0 to 15% buffer B, and a 130-min gradient from 15 to 45% buffer B, followed by a 20-min gradient increase to 100% buffer B and a reverse of the gradient to 100% buffer A. The 5-min buffer C percentages (*X*) were 30, 70, and 100%. As peptides were eluted from the microcapillary column, they were electrosprayed directly into an LTQ linear ion trap (Thermo) with the application of a distal 2.4-kV spray voltage. A cycle of one full-scan mass spectrum (400 to 1,400 *m*/*z*) was followed by three data-dependent tandem mass spectrometry spectra at a 35% normalized collision energy. Tandem mass spectrometry spectra for peptides were analyzed by using the following software analysis protocol. Poor-quality spectra were removed from the data set by using an automated spectral quality assessment algorithm (3). Tandem mass spectrometry spectra remaining after filtering were searched with the SEQUEST algorithm against a database concatenated to a decoy database in which the sequence for each entry in the original database was reversed (9). No enzyme specificity was considered for any search. SEQUEST results were assembled and filtered by using the DTASelect program (version 2.0) (42). DTASelect 2.0 uses a linear discriminant analysis to dynamically set XCorr and DeltaCN thresholds for the entire data set to achieve a user-specified false-positive rate (5% in this analysis).

Measurement of IGF-II in conditioned medium. Conditioned media were collected from shCtrl and shNET39#2 C2C12 cells 1 day after the shift to differentiation conditions and were concentrated 20-fold with Microcon YM-3 columns (Millipore). The proteins in the media were examined by immunoblotting using the anti-IGF-II antibody.

IGF-II–muscle-specific enhancer (ME) reporter assay. C2C12 cells were transfected with H19-luc-ME (11) and allowed to reach confluence for 24 h. The cells were then switched to DM. At various time points, cell lysates were collected and analyzed for luciferase activity, using a luciferase assay system kit (Promega) following the manufacturer's protocol (27).

RESULTS

NET39 is an NE-enriched transmembrane protein belonging to the LPP family but has no detectable enzymatic activity. NET39 (Ppapdc3) is an NE transmembrane protein of 271 amino acids that we originally identified by proteomic analysis of isolated NEs (38). The Ppapcd3 gene encodes an as yet uncharacterized member of the LPP family. It is upregulated over 40-fold at the transcriptional level during myogenesis in culture (6). When overexpressed in C2C12 cells (6) or HeLa cells (38) (Fig. 1A), NET39 becomes concentrated at the NE and also is present in a peripheral ER-like localization, as commonly seen for other overexpressed NE transmembrane proteins. An evaluation of the membrane orientation of NET39 using the program TMHMM, version 2.0 (http://www.cbs.dtu.dk), predicted that NET39 contains a hydrophilic domain of about 100 residues at its N terminus, followed by four transmembrane segments extending to the C terminus (Fig. 1B). The transmembrane orientation predicted for NET39 is different from that described for other members of the LPP family, which have six predicted transmembrane regions (40).

We used indirect immunofluorescence to map the transmembrane topology of the N and C termini of NET39, using HeLa cells transfected with NET39 containing an N-terminal Myc epitope tag or a C-terminal V5 epitope tag. Both epitopes were detected in ER-like membranes when fixed cells were permeabilized with 0.2% Triton X-100, which perforates all cellular membranes (Fig. 1A). Both epitopes also were accessible when the fixed cells were treated with 30 μg/ml digitonin, which selectively breaches the plasma membrane but leaves ER membranes intact (1), as evidenced by the inaccessibility of the ER luminal protein PDI (Fig. 1A). However, the pronounced nuclear rim staining of NET39 seen with Triton treatment was conspicuously absent with digitonin permeabilization, supporting the notion the most NE staining arises from NET39 localized at the INM (which is inaccessible to antibodies in digitonin-permeabilized cells) (1). Thus, both the N and C termini of NET39 are exposed to the cytosol/nucleoplasm (Fig. 1A and B). NET39 in transfected cells remains nuclear rim associated after Triton preextraction (6), supporting the notion that it physically interacts with the Triton-insoluble nuclear lamina. We found that the hydrophilic N terminus of NET39 is not necessary for its Triton-resistant targeting to the NE, because a construct lacking the N-terminal 91 amino acids was still targeted to the nuclear rim and colocalized with lamins A/C, similar to the full-length protein (Fig. 1B and C).

Gene database searches showed that NET39 is highly conserved in mammals; the human and mouse proteins are >95% identical. It also revealed homologous proteins in *Xenopus* and zebrafish (Fig. 2 and data not shown). However, no proteins with significant homology could be found in *Drosophila* or other invertebrates. Unlike other LPP family members, NET39 lacks certain of the highly conserved residues implicated in phosphatase activity (40). Alignment with the invariant tripartite consensus sequences (denoted C1, C2, and C3) that define LPPs (e.g., LPP3 and Ppapdc2) revealed nonconservative substitutions in NET39 at three residues that are thought to be critical in catalysis (Fig. 2A) (40).

To directly examine whether NET39 is an LPP, we examined whether recombinant V5-tagged NET39 that was immunoadsorbed from nonionic detergent lysates of transfected HEK293A cells had catalytic activity against a select group of potential substrates (Fig. 2B). We detected no phosphatase activity against Triton X-100-solubilized PA, LPA, C1P, S1P, DGPP, or FDP. In contrast, recombinant LPP3-V5 prepared in a similar manner showed substantial phosphatase activity against PA, LPA, and DGPP (Fig. 2B), as reported previously (17, 23). Interestingly, coimmunoprecipitation experiments indicated that Myc-NET39 is directly or indirectly associated with NET39-V5 and with LPP3-V5 in transfected cells (Fig. 2C), suggesting that NET39 may exist in homo- and/or heterooligomers in its native cellular context. This property has been reported previously for LPP1, LPP2, and LPP3 (28). Furthermore, Blue Native polyacrylamide gel electrophoresis experi-

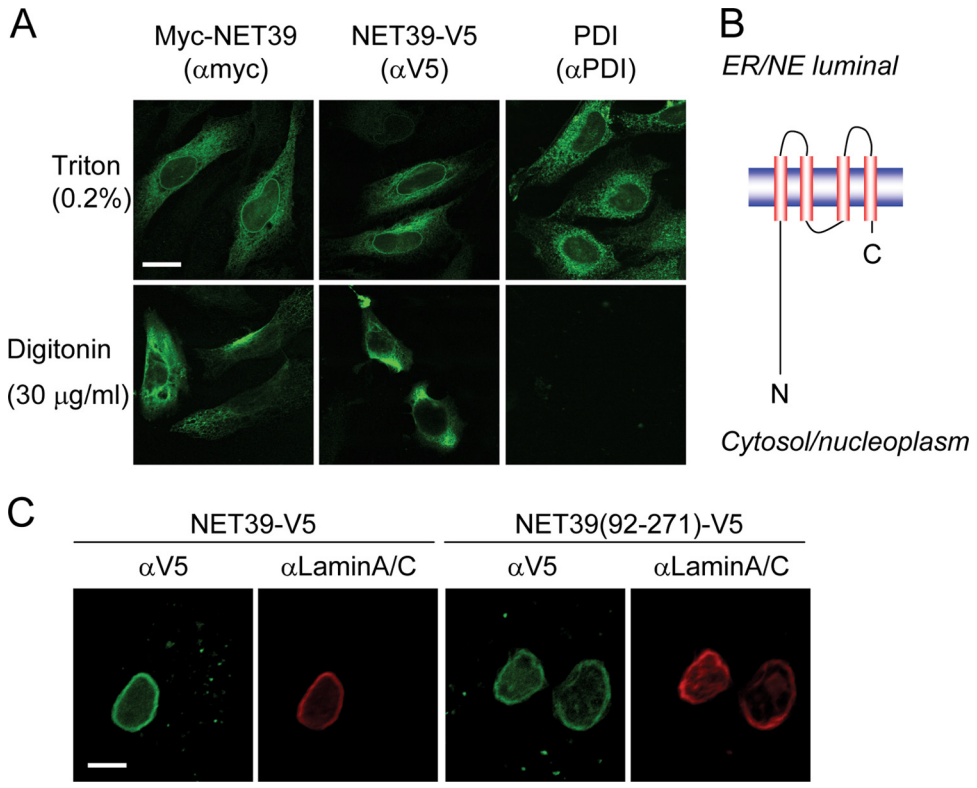

FIG. 1. Localization and membrane topology of NET39. (A) HeLa cells transiently expressing Myc-NET39 or NET39-V5 were fixed with 4% formaldehyde and then treated with 0.2% Triton to permeabilize all cellular membranes or with 30 μg/ml digitonin to selectively permeabilize the plasma membrane. Cells were then incubated with anti-Myc or anti-V5 antibodies to visualize the epitope tags or with anti-PDI. Bar, 10 μm. (B) Model depicting the membrane topology of NET39. NET39 is predicted to have four transmembrane domains, and both the N and C termini are oriented toward the cytosol/nucleoplasm. (C) COS-7 cells transiently expressing NET39-V5 or NET39(92-271)-V5 were preextracted with 1% Triton X-100 and then were fixed with formaldehyde and analyzed by immunofluorescence staining with anti-V5 antibody. Bar, 10 μm.

ments established that both NET39 and LPP3 are present as high-molecular-weight complexes under the relatively harsh lysis conditions of Triton and 250 mM NaCl (data not shown), supporting the view that NET39 may exist in oligomers or other large protein complexes.

NET39 protein is highly expressed in striated muscle and is induced during myogenesis. To monitor endogenous NET39, we generated an affinity-purified antibody against its N-terminal hydrophilic domain. By immunoblotting, this antibody specifically recognized untagged NET39 that was overexpressed in HEK293A cells and NET39-V5 that was immunopurified with an anti-V5 antibody (Fig. 3A). Using this antibody to analyze various mouse tissues by immunoblotting, we observed that the NET39 protein is expressed at high levels in the muscle and heart compared to the brain and is nearly undetectable in the liver (Fig. 3B). This pattern was consistent with our previous quantitative reverse transcription-PCR study that analyzed NET39 mRNA levels in various murine tissues (6).

We also found that the NET39 protein was strongly upregulated in two in vitro models of myogenic differentiation. One involved the C2C12 mouse myoblast cell line, which expresses myogenic commitment factors, including MyoD. Upon removal of growth factors from confluent C2C12 cultures, cells efficiently differentiate into multinucleated myotubes (34). The other myogenic model utilized the CH3-10T1/2 mesenchymal stem cell line, which is converted to myoblasts by overexpression of MyoD and differentiates to myotubes by a subsequent shift to low-serum medium (7). When cultures of C2C12 myoblasts were induced to differentiate, small multinucleated myotubes expressing MyHC were evident 2 days after the shift, and the myotubes increased in size and number at 3 days and later (Fig. 4B). Before differentiation, the NET39 protein was expressed at a very low level (Fig. 3C and 4A). After 1 day in DM, the NET39 protein was detectably upregulated, and it was markedly upregulated at day 2 and later (Fig. 3C). The pattern of NET39 upregulation during the course of C2C12 differentiation paralleled the increase of the myogenic differentiation marker myogenin but preceded the expression wave of MyHC, a transcriptional target of myogenin (Fig. 3C). For CH3-10T1/2 cells, NET39 was clearly expressed in MyoD-transformed populations 2 days after the switch to DM (Fig. 3D), further supporting a dramatic induction of NET39 during myogenic differentiation. In immunofluorescently stained C2C12 cultures 4 days after the shift to DM, NET39 was clearly concentrated at the NE in differentiated myotubes, as marked by the localization of lamins A/C. Moreover, NET39 also was detectable in peripheral ER-like structures (Fig. 3E). In undifferentiated cells in the same cultures, lamins A/C, but not NET39, were strongly evident at the NE (Fig. 3E).

We prepared nuclear and peripheral ER membrane fractions from differentiated C2C12 cells and examined these by immunoblot analysis, using H2B and calnexin, respectively, as

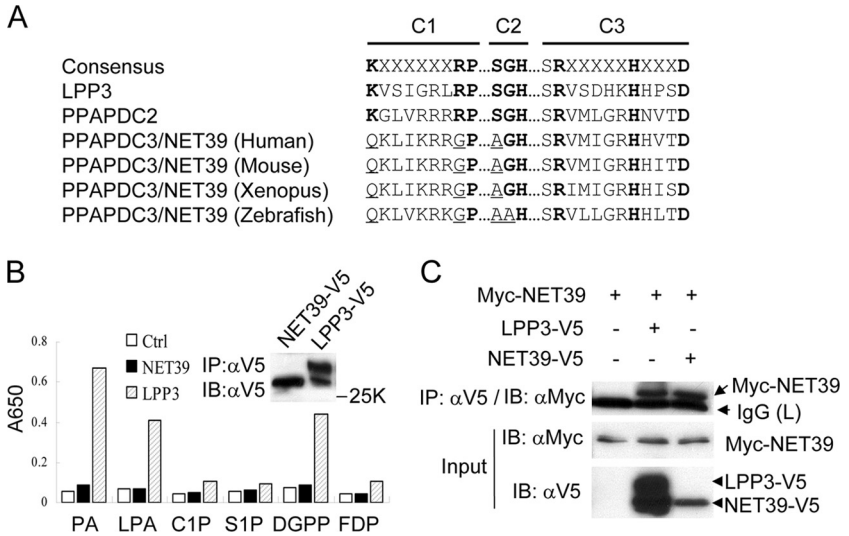

FIG. 2. NET39 is a member of the LPP family but demonstrates no detectable enzymatic activity. (A) Alignment of catalytic domain sequences of members of the LPP family. Conserved residues in the C1, C2, and C3 domains previously reported to be critical for enzyme activity are marked in bold. Ppapdc3 is the gene name for NET39. (B) Recombinant NET39-V5 and LPP3-V5 proteins were separately purified from transiently transfected HEK293A cells by immunoadsorption to anti-V5 agarose. Cells transfected with the empty vector pcDNA3 were also employed for immunoadsorption as a negative control. Phosphatase activities of immunopurified NET39 and LPP3 proteins were measured by the malachite green assay, using either PA, LPA, C1P, S1P, DGPP, or FDP as the substrate. An immunoblot (inset) shows that the amounts of purified NET39 and LPP3 used in these assays were comparable. (C) HEK293A cells were transfected with Myc-NET39, together with or without NET39-V5 or LPP3-V5, as indicated. Thirty-six hours later, the cell lysates were subjected to immunoadsorption to anti-V5 agarose, followed by immunoblot detection with anti-Myc or anti-V5 antibody.

markers (Fig. 3F). H2B was mostly restricted to the nuclear fraction, whereas NET39 was detected in both nuclear and peripheral ER fractions. After normalizing to the ER transmembrane marker calnexin, which is equally abundant in both the NE and peripheral ER because of the physical continuity of these membranes, we found that NET39 was ~3.3-fold enriched in the nuclear (NE) fraction compared to the peripheral ER. This result agrees with the immunofluorescence analysis (Fig. 3E).

NET39 levels control myoblast differentiation. To examine a potential role of NET39 in myogenesis, we created C2C12 cell populations stably transfected with expression constructs encoding shRNAs designed to knock down NET39 expression and analyzed the ability of these cells to differentiate. We prepared cells stably expressing each of three independent shRNAs targeting the NET39 gene, as well as control cells expressing a nontargeting hairpin sequence. Of the NET39-targeting sequences analyzed, shRNAs 2 and 3 significantly reduced the (already low) protein level of NET39 in confluent myoblast cultures, whereas shRNA 4 was ineffective at NET39 silencing (Fig. 4A).

Because the expression of NET39 paralleled that of myogenin, we predicted that silencing of NET39 might delay or block late events of myogenesis, such as cell fusion and expression of MyHC. In contrast to our predictions, cells expressing either shRNA 2 or 3 showed dramatically accelerated myogenic differentiation compared to that of controls following the shift to DM, as evaluated by visualizing MyHC-positive myotubes. At day 2, cultures transfected with either control shRNA or the silencing-ineffective shNET39#4 (Fig. 4A) were at early stages of differentiation and had a myogenic index (% of nuclei in MyHC-positive cells) of <20%. In contrast, cultures transfected with shNET39#2 and shNET39#3 displayed high levels of differentiation, with the myogenic index exceeding 60% (Fig. 4B and C and data not shown). By day 3, the shNET39 cells developed into huge myotubes containing hundreds of nuclei (arrows), and nearly 90% of the nuclei were in MyHC-positive cells (Fig. 4B and C). Control differentiated C2C12 cultures never showed such gigantic myotubes, and the myogenic index typically did not exceed ~50%. This difference presumably reflects the vigorous, dysregulated myogenic signaling present in the shNET39 cultures (see below).

To complement the silencing analysis, we investigated the effects of NET39 overexpression on myogenesis. For this purpose, C2C12 myoblasts were transduced either with adenovirus-Myc-NET39 or with a control adenovirus carrying an empty cytomegalovirus cassette and then shifted to DM. In contrast to the NET39 knockdown, NET39 overexpression substantially inhibited C2C12 differentiation, as the myogenic index was reduced from 29% in controls to ~12% at day 3 (Fig. 4D and E). In further experiments, the effects of knockdown or overexpression of NET39 were examined in CH3-10T1/2 cells transduced with MyoD via adenovirus to induce myogenesis. Consistent with the results for C2C12 cells, myogenic transformation was enhanced by simultaneous transduction of the adenovirus vector encoding NET39 shRNA together with the adenovirus MyoD vector and was repressed by cotransduction with the NET39 expression vector (data not shown). Together, these data indicate that NET39 antagonizes differentiation in these myoblast models.

Proteomic screen identifies mTOR as a NET39 binding partner. Since NET39 negatively regulates myogenic differentiation, we hypothesized that it may interact with a signaling component(s) that plays a critical role in this process. To iden-

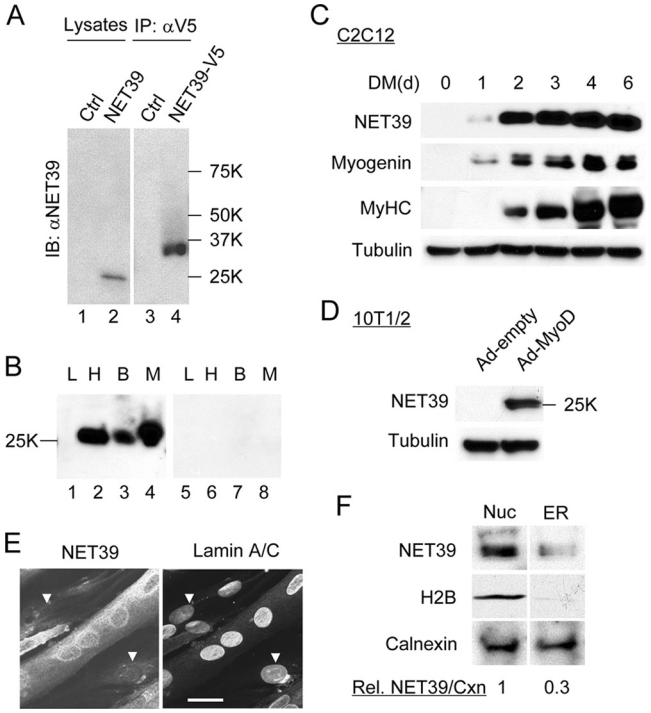

FIG. 3. NET39 is present at high levels in striated muscle tissue and is induced during myogenic differentiation. (A) HEK293A cells were transfected with the empty expression vector (Ctrl; lanes 1 and 3) or with vector containing a cDNA for untagged NET39 (lane 2) or for V5-tagged NET39 (lane 4). Thirty-six hours later, NET39-V5 was immunoadsorbed to anti-V5 agarose (lanes 3 and 4), and both the immunoprecipitates (lanes 3 and 4) and the whole-cell lysates (lanes 1 and 2) were subjected to immunoblot analysis with anti-NET39. (B) Thirty-microgram aliquots of protein extracts from liver (L), brain (B), heart (H), and skeletal muscle (M) of the mouse were analyzed by immunoblotting with anti-NET39 antibody preincubated with (lanes 5 to 8) or without (lanes 1 to 4) the blocking antigen. (C) C2C12 cells were differentiated as described in Materials and Methods, and lysates from undifferentiated cells (DM0) and cells analyzed 1 to 6 days after the shift to DM (DM1 to DM6) were analyzed by immunoblotting for NET39, myogenin, MyHC, and tubulin, using the corresponding antibodies. (D) Subconfluent CH3-10T1/2 cells were transduced with MyoD-encoding adenovirus or with control adenovirus and were allowed to reach confluence in 10% FBS. Cells were then switched to 2% HS for 2 days, and the levels of NET39 in cell lysates were analyzed by immunoblotting. (E) C2C12 cells were differentiated for 4 days and then subjected to immunofluorescence staining with anti-NET39 and anti-lamin A/C antibodies. Arrowheads denote some undifferentiated cells with strong staining for lamin but not for NET39. Bar, 10 μm. (F) ER and nuclear (Nuc) fractions from differentiated C2C12 myotubes (DM4) were subjected to immunoblotting with anti-NET39, anti-H2B, and anticalnexin antibodies, respectively. The relative intensities of the NET39 signal in the ER and nuclear fractions, normalized to calnexin (Cxn), are indicated.

tify potential targets of NET39, we analyzed NET39 interacting proteins in C2C12 myotubes, where NET39 is normally expressed at high levels. Aside from an increase in sensitivity of our analysis using this time point, we reasoned that potential partners of NET39 involved in muscle homeostasis (which may be related to those involved in inhibition of myogenic differentiation as well; see Discussion) would be identified. For this experiment, parallel C2C12 cultures were shifted to DM, and after 4 days, they were transduced either with adenovirus encoding Myc-NET39 or with adenovirus lacking an insert. Following another 2 days of culture, lysates were prepared from each culture and were immunoadsorbed to anti-Myc agarose. Proteins were eluted from the immunobeads and were analyzed by the highly sensitive MudPIT proteomic method (Fig. 5A) (46, 48). A total of 174 proteins were detected uniquely in the Myc-NET39 sample and were absent in the empty vector sample, representing proteins that are specifically associated with NET39, by either direct or indirect interactions (Fig. 5A and B; see Table S1 in the supplemental material). We verified that six randomly selected proteins identified in the proteomic data set (viz., lamin A/C, β-catenin, 14-3-3, α-tubulin, β-tubulin, and glyceraldehyde-3-phosphate dehydrogenase) were also detectable in immunoblots of the Myc-NET39 pull-down products but not in pull-down products with anti-Myc agarose alone (data not shown). The NET39-associated proteins are associated with multiple cellular structures and pathways, as depicted in Fig. 5B. These include nuclear functions; protein synthesis, folding, and degradation; signal transduction; cytoskeleton and motility; mitochondrial functions; ER membranes and exocytic and endocytic pathways; and other functions. It is noteworthy that among the NET39-associated proteins are lamins A/C (see Table S1 in the supplemental material), which could provide a Triton-insoluble anchoring site for NET39 in the NE (Fig. 1).

Of the broad spectrum of proteins associated with NET39 in myotubes, most are likely to be part of multiprotein complexes that interact with NET39 only via one of the complex components. Furthermore, many such "indirectly" interacting proteins may not be linked to physiological functions of NET39. In a hypothetical example, the interaction of NET39 with tubulin (see Table S1 in the supplemental material) might be physiologically specific, but a number of tubulin-interacting proteins, which occur in the pull-down samples due to association with tubulin, might not be pertinent. Establishing the physiological relevance of proteins identified in the proteomic screen will require detailed analysis of individual components. These caveats aside, the proteomic results suggest that NET39 may play a role in multiple facets of muscle cell regulation.

We focused on mTOR among the NET39 binding partners for the current study, as the mTOR–IGF-II axis is critical for initiation of myogenic differentiation in myoblasts (11), and an mTOR interaction could explain the phenotypes we observed in myoblasts with NET39 overexpression or knockdown. To confirm that mTOR is a binding partner of endogenous NET39, samples of NET39 immunoprecipitated from (untransduced) differentiated C2C12 cultures were analyzed by immunoblotting. As shown in the left panels of Fig. 6A, mTOR was detected only in the sample incubated with anti-NET39, not in the sample treated with the control antibody. Similarly, NET39 was detected only in the anti-mTOR, not control, immunoprecipitate (Fig. 6A, right panels). Furthermore, ectopically expressed NET39 interacted with mTOR in differentiated C2C12 cultures (Fig. 6B). By expressing NET39 and mTOR in HEK293A cells and carrying out immunoprecipitation, we found that amino acids 70 to 91 of NET39 are crucial for mediating the NET39-mTOR association, as both N-terminal and C-terminal fragments of NET39 containing this region (but not the C-terminal fragment lacking this segment) were able to associate with mTOR (Fig. 6C). Coexpression of

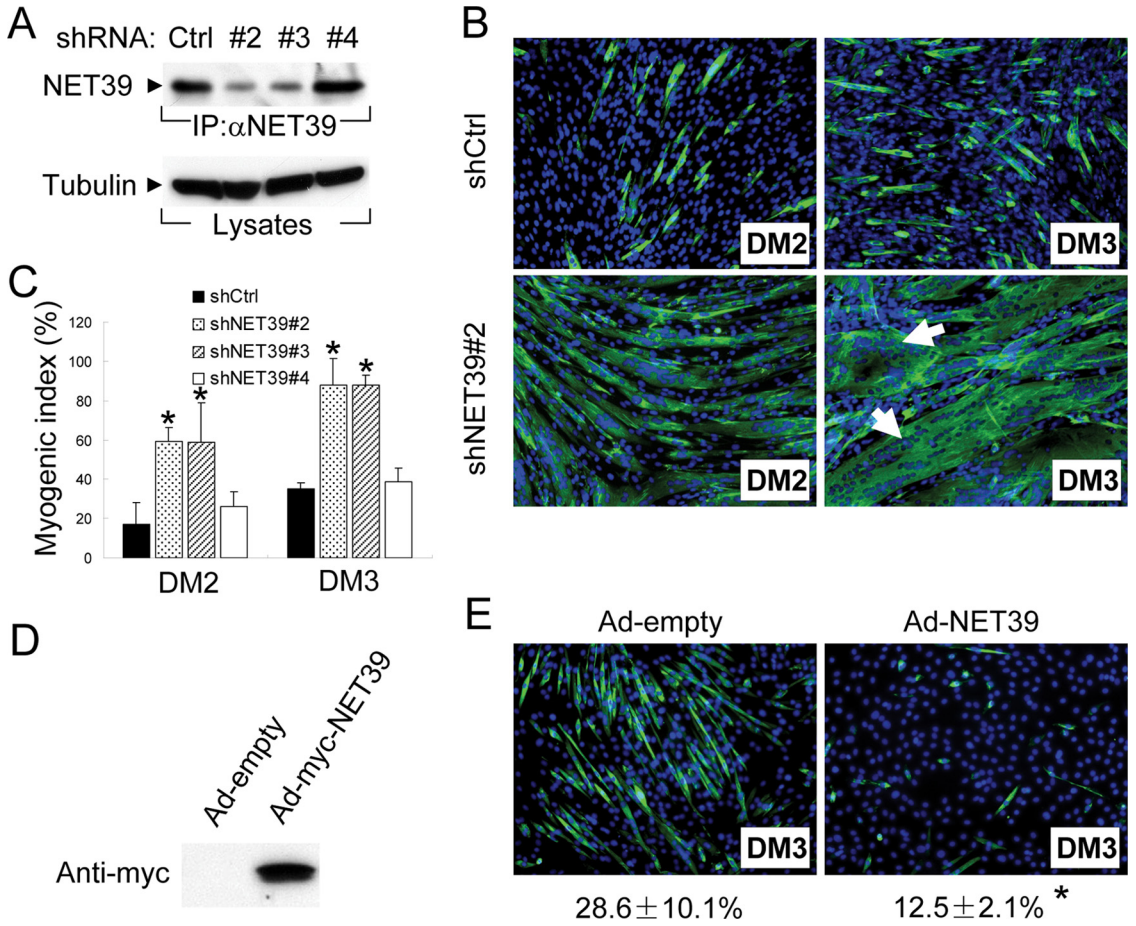

FIG. 4. NET39 antagonizes C2C12 cell myogenic differentiation. (A) Lysates containing the same amounts of protein, which were derived from separate C2C12 cultures stably expressing each of three NET39-targeting shRNAs (shRNAs 2, 3, and 4) and a nontargeting hairpin sequence (shCtrl), were subjected to immunoprecipitation with anti-NET39 antibody. The immuno-enriched NET39 protein and the tubulin in the initial lysates were analyzed by immunoblotting. (B) Micrographs showing immunofluorescence staining of C2C12 cells stably transfected with shCtrl or with shNET39#2 (green, MyHC; blue, DNA). Cultures were maintained in DM for the indicated times before analysis. Arrows denote huge multinucleated myotubes. (C) Quantification of myogenic differentiation from the experiment in panel B. The myogenic index is the percentage of nuclei in MyHC-positive cells. Error bars indicate standard deviations. (D) Immunoblot analysis, using anti-Myc antibody, of C2C12 myoblasts transduced with adenovirus expressing Myc-NET39 or with control adenovirus and examined 2 days after transduction. (E) C2C12 myoblast cultures (25% confluent) were transduced with adenovirus encoding Myc-NET39, allowed to reach confluence, and switched to DM for 3 days. Typical MyHC immunostaining and the myogenic index are shown. *, $P < 0.05$; **, $P < 0.01$.

NET39 and several mTOR fragments in HEK293A cells, followed by immunoprecipitation, revealed that both the N-terminal ~1,500 residues and C-terminal ~550 residues of mTOR are sufficient for NET39 binding (Fig. 6D). To evaluate the strength of mTOR-NET39 interaction, we treated the NET39-V5 immunoprecipitates from HEK293A cells with increasingly stringent wash conditions. A high salt concentration (1 M or 2 M KCl) and 2 M urea had no effect on the association of NET39 and endogenous mTOR, and disruption of the interaction was seen only with 4 M urea (Fig. 6E). This indicates that mTOR is tightly associated with NET39, although it cannot be excluded that this interaction is indirect. The robust interaction between NET39 and mTOR was further demonstrated by the observation that ectopic overexpression of NET39 in HeLa cells targeted endogenous mTOR from a mixed cytoplasmic and nuclear localization (Fig. 7A, middle panel, inset) to the NE and peripheral ER-like membrane localization seen for NET39 (Fig. 7A). As a control, overexpression of Myc-NET39 did not alter the localization of PDI, an ER luminal protein (Fig. 7B). Although it was feasible to localize mTOR in human cells, we were not able to obtain a suitable antibody for immunolocalization in C2C12 (murine) cells.

NET39 regulates mTOR signaling and the production of IGF-II during C2C12 cell differentiation. Since NET39 negatively regulates myogenesis in culture and interacts strongly with mTOR, we speculated that it might antagonize the action of mTOR in initiating myogenesis. We therefore examined mTOR in the early stages of C2C12 cell differentiation in cells where NET39 levels were altered by silencing or overexpression. As a proxy for evaluating the functional state of mTOR during this period, we measured the activity of mTOR as determined by the phosphorylation of its downstream target p70S6K. As shown in Fig. 8B, the expression of shNET39#2 significantly enhanced p70S6K phosphorylation, particularly at 0 h and 1 h after the shift to DM. Conversely, overexpression of NET39 strongly repressed p70S6K phosphorylation over the

A

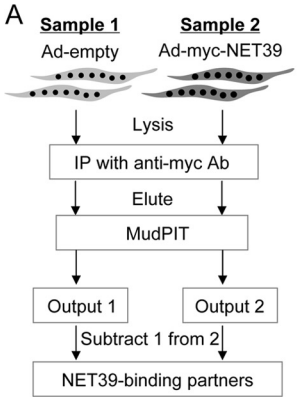

B

Classification	Hits
Nuclear functions	24
Protein synthesis/folding/degradation	37
Signal transduction	20
Cytoskeletal and contractile proteins	26
Mitochondrial functions	14
ER membrane and secretory/endocytic pathways	32
Others	20

FIG. 5. Identification of NET39-associated proteins in myotubes by MudPIT analysis. (A) C2C12 cells were incubated in DM for 4 days to induce myotube formation and then transduced either with adenovirus encoding Myc-NET39 or with control adenovirus. After another 2 days, cell lysates were prepared and subjected to immunoadsorption to anti-Myc agarose, and the bound proteins were eluted with 8 M urea. By MudPIT proteomics, 173 proteins were identified as NET39-binding partners, as they were detected in the Myc-NET39 sample but were absent in the control sample. (B) NET39-associated proteins within different functional classes.

entire 24-h window following serum withdrawal (Fig. 8A). Thus, NET39 negatively regulates the activity of mTOR during early stages of differentiation, and this correlates with the negative effects of NET39 on myogenesis. Although the kinase activity of mTOR is reported to not be required for mTOR-regulated initiation of myogenesis differentiation (10, 11), NET39 clearly could affect other functions of mTOR, as well as its activity, through its physical interaction with mTOR.

We found that the regulation of mTOR kinase activity by NET39 occurs only during the early stage of myogenic differentiation, as knockdown of NET39 by adenovirus-mediated transduction in differentiated myotube cultures at DM3 did not affect the basal and insulin-induced phosphorylation of p70S6K measured 3 days later (data not shown; also see Discussion). The detailed mechanism by which NET39 specifically regulates the kinase activity of mTOR at an early stage of myogenic differentiation and the exact relationship of this to myogenesis need to be investigated further.

mTOR signaling regulates the transcription of mRNA for IGF-II, an autocrine/paracrine factor responsible for initiating differentiation in C2C12 cells (11). To ascertain that the myogenic effect of NET39 involves the mTOR pathway, we examined whether IGF-II production was expedited upon NET39 knockdown. As shown in Fig. 8C, when myoblasts stably expressing shNET39#2 were shifted to DM, a significant amount of IGF-II was found in the medium 1 day after the shift, whereas essentially no IGF-II was present in the medium of shCtrl myoblasts at this early time point. Since mTOR signaling has been shown to regulate the transcription of the IGF-II gene through a muscle-specific enhancer (termed "ME") (11), we examined the effect of NET39 silencing on the activity of ME measured with a luciferase reporter plasmid. We found that the induction of ME activity during myogenesis was strongly enhanced by NET39 knockdown (Fig. 8D), consistent with the effects we observed on IGF-II secretion.

As an independent approach to validate that stimulation of the mTOR–IGF-II axis is responsible for the enhanced myogenesis obtained by silencing NET39, shNET39-transfected cells were shifted to DM for 1 day in the presence of rapamycin, a specific mTOR inhibitor. As shown in Fig. 8E and F, repression of mTOR by rapamycin during the first day after the shift to DM abrogated myogenesis promoted by the knockdown of NET39. A similar phenomenon was also observed in cells incubated with a combination of 1-butanol and R59022, which block the synthesis of PA, a physiological activator of mTOR (Fig. 8E and F) (15, 26, 50). Interestingly, addition of the mTOR inhibitors at DM1 did not block NET39 knockdown-facilitated myogenic differentiation (data not shown), thus suggesting that the effects of NET39 in regulating mTOR activity and myogenesis occur only at the early stage of myogenesis (see Discussion). Supporting this speculation, we also found that overexpression of NET39 by adenovirus transduction after the switch to DM (the viruses were added at DM0, DM1, DM2, or DM3) did not markedly repress the expression of myogenin (data not shown).

Next, we examined whether the addition of IGF-II could rescue the effect of mTOR repression. As shown in Fig. 8F, addition of IGF-II alone was sufficient to reverse the negative effects of rapamycin or 1-butanol plus R59022 on myotube formation in shNET39 cells, suggesting that hyperactivation of the mTOR–IGF-II axis indeed contributes to enhanced myogenesis caused by knockdown of NET39. To complement the above observations, conditioned medium from "donor" shCtrl or shNET39 cells, taken 24 h after the shift to differentiation conditions, was transferred to "recipient" C2C12 cells. As shown in Fig. 8G, the conditioned medium from shNET39 cells exerted a much stronger effect in promoting differentiation of the recipient cells than did the medium from control cells. The differentiation-promoting factor in the shNET39 medium was at least mainly IGF-II, since preincubation with an anti-IGF-II antibody, but not with a control IgG, strongly reduced the myogenic potency of the shNET39 medium (Fig. 8G). Taken together, these results suggest that NET39 likely exerts its function by controlling mTOR-dependent IGF-II expression, a critical step in the initiation of the differentiation program in myoblasts.

DISCUSSION

The kinase mTOR functions as a master regulator of cell growth, proliferation, and various types of cellular differenti-

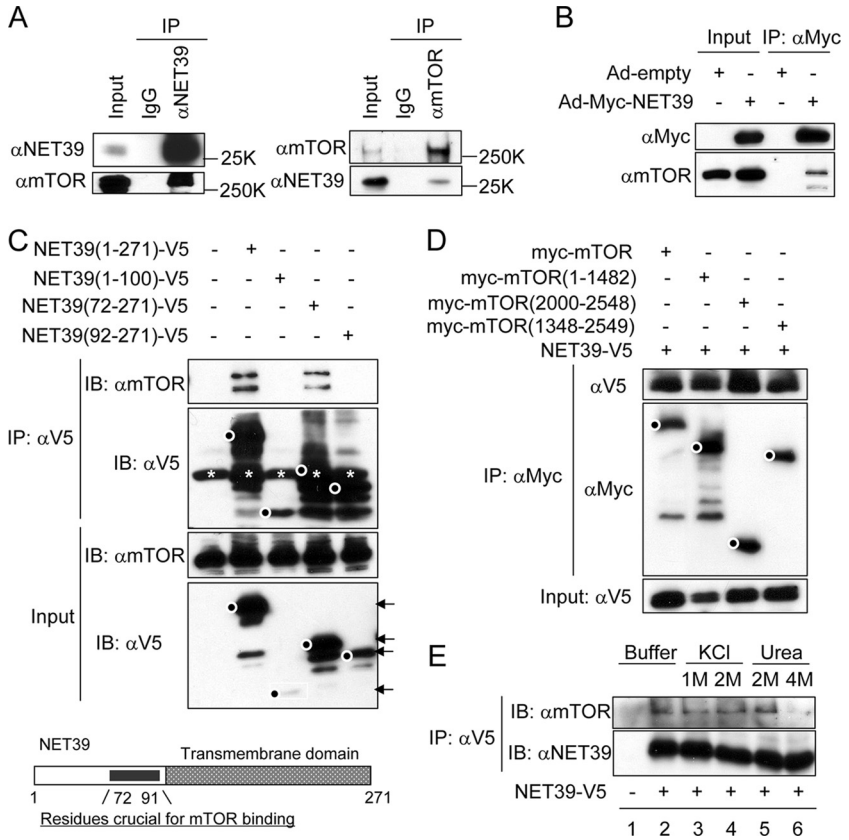

FIG. 6. Characterization of NET39-mTOR association. (A) (Left) A sample of C2C12 cells after 4 days in DM was immunoadsorbed with anti-NET39 antibody or with a control antibody, and the bound material was analyzed by immunoblotting to detect mTOR. (Right) Same as for the left panels, except that anti-mTOR antibody and a control antibody were used for immunoprecipitation. (B) C2C12 cultures were transduced after 4 days in DM with adenovirus encoding Myc-NET39 or with control adenovirus. Forty-eight hours later, the cell lysates were immunoprecipitated with anti-Myc agarose and subjected to immunoblotting with anti-Myc or anti-mTOR antibodies. (C) HEK293A cells were transfected with various V5-tagged NET39 truncation mutants, as indicated. Forty-eight hours later, the cell lysates were immunoprecipitated with anti-V5 agarose and subjected to immunoblotting with anti-V5 or anti-mTOR antibodies. Black dots denote the specific unproteolyzed polypeptides encoded by the indicated NET39 constructs, and asterisks denote the IgG light chain. (D) HEK293A cells were transfected with NET39-V5 and various Myc-tagged mTOR truncation mutants, as indicated. Forty-eight hours later, the cell lysates were immunoprecipitated with anti-Myc agarose and subjected to immunoblotting with anti-Myc or anti-V5 antibodies. Black dots denote the specific unproteolyzed polypeptides encoded by the indicated mTOR constructs. (E) HEK293A cells were transfected with NET39-V5 (lanes 2 to 6) or with empty vector (lane 1), and after 36 h, cell lysates were prepared and subjected to immunoadsorption to anti-V5 agarose. After three washes with immunoprecipitation buffer, the immunoprecipitates were washed another time with either Tris buffer (50 mM Tris-HCl, pH 7.5, 50 mM NaCl) (lanes 1 and 2) or Tris buffer containing 1 M or 2 M KCl (lanes 3 and 4) or 2 M or 4 M urea (lanes 5 and 6). The immunoadsorbent beads were then subjected to immunoblot analysis.

ation by sensing nutrient availability and cellular energy levels (20). For myogenesis in cultured cells, mTOR regulates IGF-II transcription in response to amino acid signaling, and this is critical for initiation of myogenic differentiation (11). Up to now, little is known about how the mTOR–IGF-II pathway is regulated during myogenesis. Here we show that the NE protein NET39 associates with mTOR and represses mTOR–IGF-II signaling during myoblast differentiation. The NET39-mTOR interaction is robust, since we detected it in cell lysates after solubilization under stringent conditions (i.e., nonionic detergent and 250 mM NaCl, which dissociates the mTORC components raptor and rictor from mTOR [25]), and we found that the association persisted in 2 M salt and 2 M urea. Using the kinase activity of mTOR as a proxy for its functional state, we found that knockdown of NET39 enhanced the activity of mTOR at the onset of C2C12 cell differentiation, as indicated by p70S6K phosphorylation, and accelerated the production and secretion of the critical autocrine/paracrine factor IGF-II. Conversely, overexpression of NET39 repressed mTOR activity upon a shift of cells to differentiation conditions.

It should be pointed out that the function of mTOR during myoblast differentiation as a signaling factor upstream of IGF-II transcription (11, 49, 50) is at least partially distinct from its functions in mature myotubes, where it can mediate IGF-I-induced hypertrophy by serving as a key downstream kinase (37). The mTOR–IGF-II axis serves as a distinctive initiator of myogenic differentiation that plays a crucial role only in the early stage of myogenesis, since inactivation of mTOR by rapamycin at DM2 is not able to abolish myogenesis (35). These results are very similar to our finding that NET39 influences myogenesis only at an early stage of differentiation. Intriguingly, the kinase activity of mTOR is reported not to be

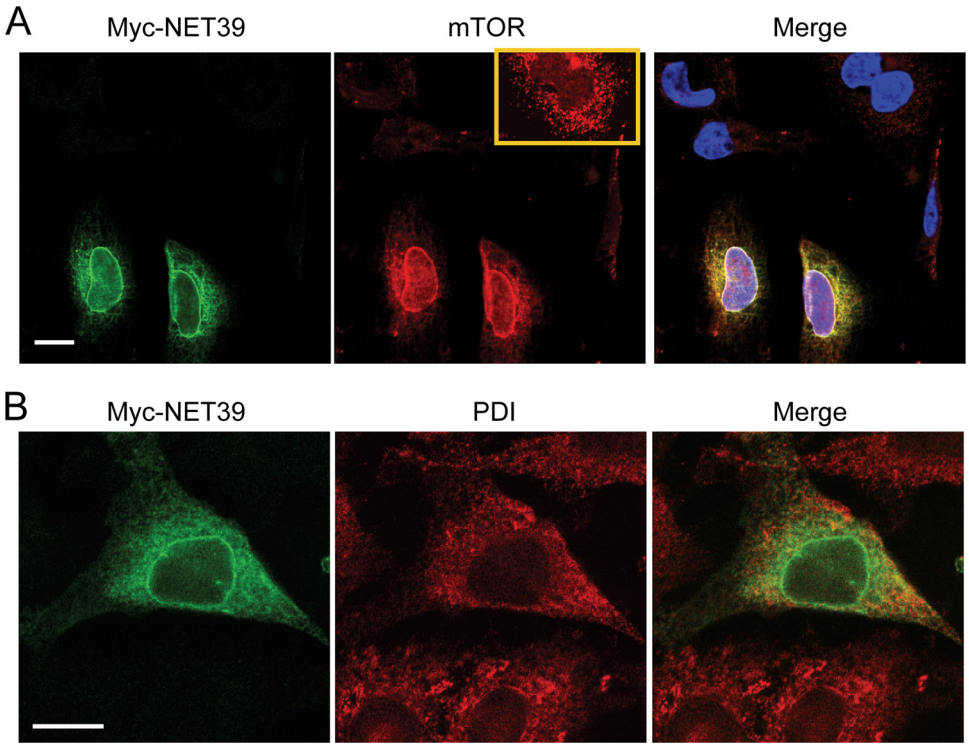

FIG. 7. Ectopic overexpression of NET39 in HeLa cells targets mTOR to the NE. (A) HeLa cells were transiently transfected with Myc-NET39, and after 48 h, cells were immunostained with anti-mTOR and anti-Myc antibodies. The stronger mTOR signal in transfected cells suggests that expression of NET39 increases the epitope accessibility for the anti-mTOR antibody, since the level of mTOR protein in the transfected cultures was unchanged, as determined by immunoblotting (data not shown). The inset presents an image of a nontransfected cell whose fluorescence intensity is digitally enhanced compared to the rest of the image, to more clearly reveal the mTOR localization in the absence of ectopic NET39. (B) HeLa cells were transiently transfected with Myc-NET39, and after 48 h, cells were immunostained with anti-PDI and anti-Myc antibodies. Bar, 10 μm.

required for mTOR-regulated myoblast differentiation, although the exact mechanism by which mTOR regulates transcription of IGF-II needs to be determined (10, 11). Since mTOR is localized mainly in the nucleus in C2C12 myoblasts (51), NET39 may recruit mTOR to the INM. This may serve as a physical sequestration mechanism to limit the availability of mTOR in control of IGF-II transcription (11), and the upregulation of NET39 may therefore impose negative feedback for a precisely tuned regulation of myogenesis. Indeed, physical sequestration of transcriptional regulators at the NE as a means of inhibiting their activity has been described previously (18, 21). It is plausible that the NET39-mTOR interaction is regulated by specific posttranslational modifications (on NET39 and/or mTOR) which appear or function only during the period of cell cycle exit.

NET39 is the only known member of the LPP family that is localized at the NE. We could not detect phosphatase activity of NET39 toward common phospholipid substrates. These results, combined with the observation that NET39 contains nonconservative substitutions in presumptive key catalytic site residues, suggest that NET39 may be a phosphatase-dead variant. In a similar vein, NET39 also has been proposed to be a candidate type 2 sphingomyelin synthase, but a recent study indicated that it does not have this enzyme activity (22). The LPP family member most closely related to NET39 that shows LPP activity, Ppapdc2, contains intact phosphatase motifs (17). Nonetheless, we cannot exclude the possibility that NET39 serves as a phosphatase for an unknown lipid substrate and regulates lipid signaling in the nucleus. Interestingly, LPP3 has been reported to repress β-catenin-mediated transcription and axis duplication in a phosphatase-independent manner (12). This report, together with our findings, implies that some LPP family members, including NET39, exert some of their functions in a manner independent of lipid signaling.

The strong transcriptional upregulation of NET39 during myogenesis likely is controlled by early myogenic regulatory transcription factors, such as MyoD or MEF2. Consistent with this notion, the upregulation of NET39 parallels that of myogenin, another MyoD/MEF2 target. MEF2, which is selectively active in brain as well as in muscle, also may control the expression of NET39 that is observed in the former tissue. Interestingly, HDAC9 was recently identified as an MEF2 target gene (19). Since HDAC9 serves as a corepressor of MEF2, upregulation of HDAC9 during myogenesis might serve as a negative feedback mechanism to limit myogenic gene expression (19). NET39 may be part of an additional negative feedback mechanism, because it has the ability to inhibit expression of myogenic genes by the mTOR-IGF2 pathway, and potentially by other pathways (see the following paragraph).

Although we have focused mainly on regulation of the mTOR–IGF-II pathway by NET39 in this study, other NET39-binding partners identified in our proteomic screen also may

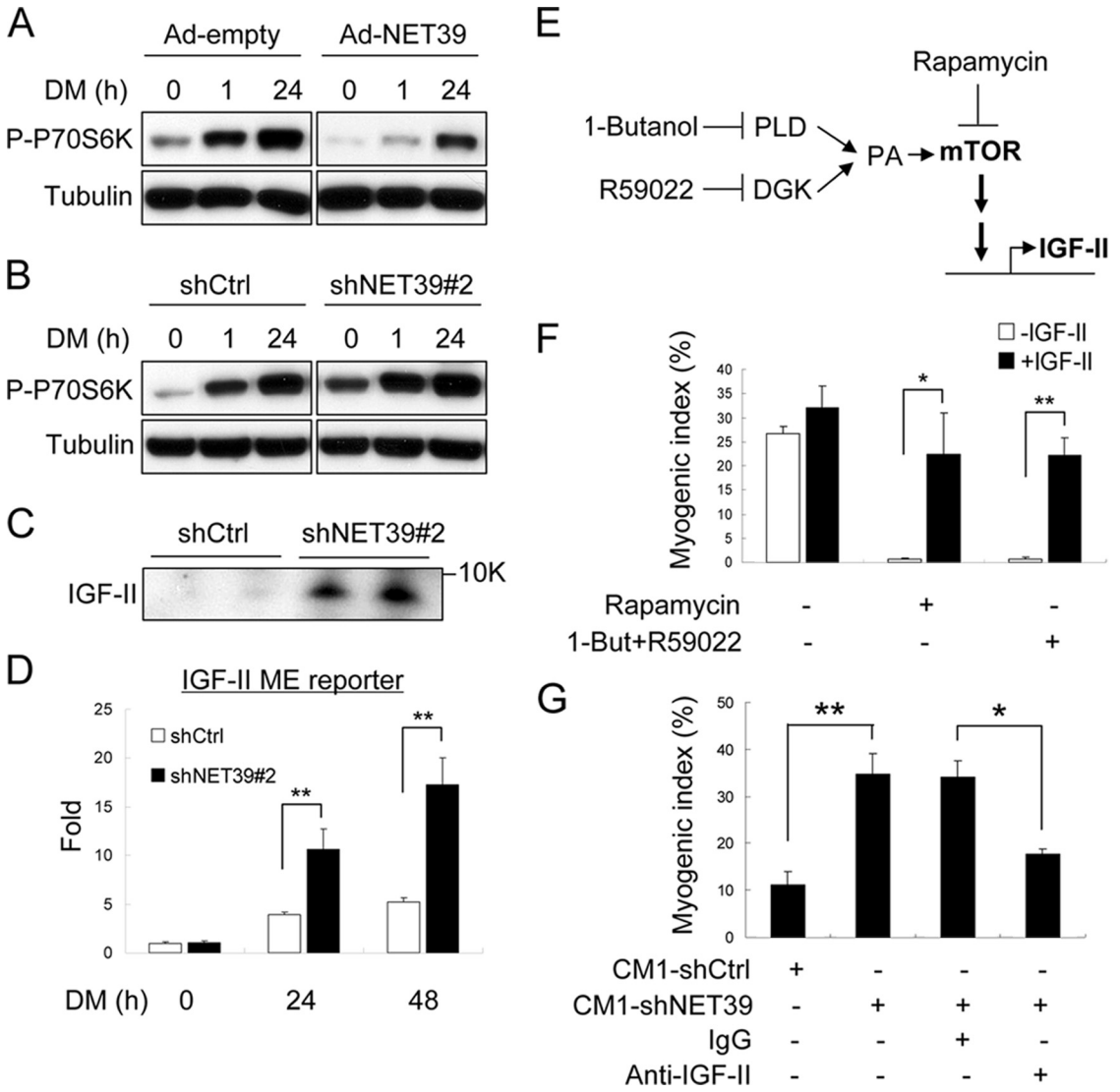

FIG. 8. NET39 negatively regulates the mTOR–IGF-II pathway during myogenesis. (A) C2C12 myoblast cultures at 25% confluence were transduced with adenovirus encoding Myc-NET39, allowed to reach confluence, and switched to DM for the indicated times. The expression of phosphorylated p70S6K and tubulin was determined by immunoblotting. (B) C2C12 cells stably expressing shNET39#2 were switched to DM for the indicated times, and levels of phosphorylated p70S6K and tubulin were determined by immunoblotting. (C) IGF-II in the medium from shCtrl or shNET39#2 C2C12 cells 24 h after the shift to differentiation conditions was assessed by immunoblotting with anti-IGF-II antibody. Blots show duplicate independent samples. (D) C2C12 cells stably expressing shCtrl or shNET39#2 were transfected with the H19-luc-ME reporter and induced to differentiate. At the indicated times, cells were lysed and luciferase assays were performed. Standard deviations are shown. (E) Diagram showing pathways for repression of mTOR activity by the pharmacological inhibitors used in panels F and G. Both phospholipase D (PLD) and diacylglycerol kinases (DGKs) can catalyze the production of PA, a physiological activator of mTOR. 1-Butanol and R59022 are specific inhibitors of PLD and DGKs, respectively. Rapamycin is a specific inhibitor of mTOR. (F) shNET39#2 C2C12 cells were differentiated for 1 day in the presence or absence of rapamycin (mTOR inhibitor) or the combination of 1-butanol (a PLD inhibitor) and R59022 (a DGK inhibitor), with or without 150 ng/ml recombinant IGF-II. Myotube formation was assessed by MyHC staining, and myogenic indexes are shown. (G) Donor cells (shCtrl and shNET39#2 cells) were shifted to DM for 24 h, and the media were harvested. These media ("CM1") then were transferred to the recipient cells in the presence of an anti-IGF-II blocking antibody or a control IgG. The recipient cells were stained for MyHC after 24 h, and myogenic indexes were determined. *, $P < 0.05$; **, $P < 0.01$.

contribute to NET39 regulation of myogenesis. Among the binding partners we identified, we currently are analyzing β-catenin and TIP120B, which were recently reported to activate MyoD and myogenin, respectively (24, 39). Moreover, β-catenin is known to be required for early myogenic differentiation (4).

In this study, we observed a potent modulation of myogenic differentiation by silencing or overexpression of NET39 in myoblasts, where it normally is expressed at only low levels. NET39 is expressed at much higher levels after myoblast differentiation and in mature muscle. We predict that NET39 will engage in conceptually similar physiological regulation in the latter biological contexts. In this case, we propose that NET39 functions are linked to muscle homeostasis in both normal and

pathological muscle regeneration. Such functions could be particularly important in the heart, where pathological hypertrophy is a major human health issue. It is conceivable that genetic defects in human NET39 might be manifest as pathological cardiac hypertrophy. We are constructing a mouse model for conditional disruption of NET39 to directly test this hypothesis.

A close involvement of NET39 in muscle homeostasis is supported by data from a recently published study on muscle regeneration in the mouse (29). It was found that the mRNA of NET39 in experimentally damaged mouse muscle was strongly diminished 3 days after cardiotoxin administration, whereas the expression of mTOR was not affected. The decreased expression of NET39 correlated with transcriptional upregulation of IGF-II, the mTOR-regulated autocrine gene, as well as with upregulation of MyoD and myogenin. This animal study supports our observations with cultured cells showing that NET39 negatively regulates myogenesis by counteracting the mTOR–IGF-II pathway. As outlined above, it is plausible, if not likely, that NET39 regulates additional homeostatic pathways in muscle. The list of potential NET39 targets we identified by proteomics in this study, which include structural/contractile proteins, ER membrane proteins, and proteins involved in apoptosis, will provide a valuable framework for future studies addressing this question.

ACKNOWLEDGMENTS

We are grateful to Do-Hyung Kim (University of Minnesota) and Jie Chen (University of Illinois at Urbana-Champaign) for generously providing plasmids.

This work was supported by NIH grant GM28521 to L.G. and by NIH grants P41 RR011823 and R01 HL079442 to J.R.Y.

REFERENCES

1. **Adam, S. A., R. S. Marr, and L. Gerace.** 1990. Nuclear protein import in permeabilized mammalian cells requires soluble cytoplasmic factors. J. Cell Biol. **111:**807–816.
2. **Bengtsson, L.** 2007. What MAN1 does to the Smads. TGFbeta/BMP signaling and the nuclear envelope. FEBS J. **274:**1374–1382.
3. **Bern, M., D. Goldberg, W. H. McDonald, and J. R. Yates III.** 2004. Automatic quality assessment of peptide tandem mass spectra. Bioinformatics **20**(Suppl. 1)**:**i49–i54.
4. **Brack, A. S., I. M. Conboy, M. J. Conboy, J. Shen, and T. A. Rando.** 2008. A temporal switch from notch to Wnt signaling in muscle stem cells is necessary for normal adult myogenesis. Cell Stem Cell **2:**50–59.
5. **Charge, S. B., and M. A. Rudnicki.** 2004. Cellular and molecular regulation of muscle regeneration. Physiol. Rev. **84:**209–238.
6. **Chen, I. H., M. Huber, T. Guan, A. Bubeck, and L. Gerace.** 2006. Nuclear envelope transmembrane proteins (NETs) that are up-regulated during myogenesis. BMC Cell Biol. **7:**38.
7. **Davis, R. L., H. Weintraub, and A. B. Lassar.** 1987. Expression of a single transfected cDNA converts fibroblasts to myoblasts. Cell **51:**987–1000.
8. **Dorner, D., J. Gotzmann, and R. Foisner.** 2007. Nucleoplasmic lamins and their interaction partners, LAP2alpha, Rb, and BAF, in transcriptional regulation. FEBS J. **274:**1362–1373.
9. **Eng, J., A. McCormack, and J. Yates.** 1994. An approach to correlate tandem mass spectral data of peptides with amino acid sequences in a protein database. J. Am. Soc. Mass Spectrom. **5:**976–989.
10. **Erbay, E., and J. Chen.** 2001. The mammalian target of rapamycin regulates C2C12 myogenesis via a kinase-independent mechanism. J. Biol. Chem. **276:**36079–36082.
11. **Erbay, E., I. H. Park, P. D. Nuzzi, C. J. Schoenherr, and J. Chen.** 2003. IGF-II transcription in skeletal myogenesis is controlled by mTOR and nutrients. J. Cell Biol. **163:**931–936.
12. **Escalante-Alcalde, D., L. Hernandez, H. Le Stunff, R. Maeda, H. S. Lee, J.-G. Cheng, V. A. Sciorra, I. Daar, S. Spiegel, A. J. Morris, and C. L. Stewart.** 2003. The lipid phosphatase LPP3 regulates extra-embryonic vasculogenesis and axis patterning. Development **130:**4623–4637.
13. **Florini, J. R., D. Z. Ewton, and K. A. Magri.** 1991. Hormones, growth factors, and myogenic differentiation. Annu. Rev. Physiol. **53:**201–216.
14. **Florini, J. R., K. A. Magri, D. Z. Ewton, P. L. James, K. Grindstaff, and P. S. Rotwein.** 1991. "Spontaneous" differentiation of skeletal myoblasts is dependent upon autocrine secretion of insulin-like growth factor-II. J. Biol. Chem. **266:**15917–15923.
15. **Foster, D. A.** 2007. Regulation of mTOR by phosphatidic acid? Cancer Res. **67:**1–4.
16. **Frock, R. L., B. A. Kudlow, A. M. Evans, S. A. Jameson, S. D. Hauschka, and B. K. Kennedy.** 2006. Lamin A/C and emerin are critical for skeletal muscle satellite cell differentiation. Genes Dev. **20:**486–500.
17. **Fukunaga, K., M. Arita, M. Takahashi, A. J. Morris, M. Pfeffer, and B. D. Levy.** 2006. Identification and functional characterization of a presqualene diphosphate phosphatase. J. Biol. Chem. **281:**9490–9497.
18. **Gonzalez, J. M., A. Navarro-Puche, B. Casar, P. Crespo, and V. Andres.** 2008. Fast regulation of AP-1 activity through interaction of lamin A/C, ERK1/2, and c-Fos at the nuclear envelope. J. Cell Biol. **183:**653–666.
19. **Haberland, M., M. A. Arnold, J. McAnally, D. Phan, Y. Kim, and E. N. Olson.** 2007. Regulation of HDAC9 gene expression by MEF2 establishes a negative-feedback loop in the transcriptional circuitry of muscle differentiation. Mol. Cell. Biol. **27:**518–525.
20. **Hay, N., and N. Sonenberg.** 2004. Upstream and downstream of mTOR. Genes Dev. **18:**1926–1945.
21. **Heessen, S., and M. Fornerod.** 2007. The inner nuclear envelope as a transcription factor resting place. EMBO Rep. **8:**914–919.
22. **Huitema, K., J. van den Dikkenberg, J. F. Brouwers, and J. C. Holthuis.** 2004. Identification of a family of animal sphingomyelin synthases. EMBO J. **23:**33–44.
23. **Kai, M., I. Wada, S. Imai, F. Sakane, and H. Kanoh.** 1997. Cloning and characterization of two human isozymes of Mg2+-independent phosphatidic acid phosphatase. J. Biol. Chem. **272:**24572–24578.
24. **Kim, C. H., H. Neiswender, E. J. Baik, W. C. Xiong, and L. Mei.** 2008. Beta-catenin interacts with MyoD and regulates its transcription activity. Mol. Cell. Biol. **28:**2941–2951.
25. **Kim, D. H., D. D. Sarbassov, S. M. Ali, J. E. King, R. R. Latek, H. Erdjument-Bromage, P. Tempst, and D. M. Sabatini.** 2002. mTOR interacts with raptor to form a nutrient-sensitive complex that signals to the cell growth machinery. Cell **110:**163–175.
26. **Laxalt, A. M., N. Raho, A. T. Have, and L. Lamattina.** 2007. Nitric oxide is critical for inducing phosphatidic acid accumulation in xylanase-elicited tomato cells. J. Biol. Chem. **282:**21160–21168.
27. **Liu, G. H., J. Qu, and X. Shen.** 2008. NF-kappaB/p65 antagonizes Nrf2-ARE pathway by depriving CBP from Nrf2 and facilitating recruitment of HDAC3 to MafK. Biochim. Biophys. Acta **1783:**713–727.
28. **Long, J. S., N. J. Pyne, and S. Pyne.** 2008. Lipid phosphate phosphatases form homo- and hetero-oligomers: catalytic competency, subcellular distribution and function. Biochem. J. **411:**371–377.
29. **Melcon, G., S. Kozlov, D. A. Cutler, T. Sullivan, L. Hernandez, P. Zhao, S. Mitchell, G. Nader, M. Bakay, J. N. Rottman, E. P. Hoffman, and C. L. Stewart.** 2006. Loss of emerin at the nuclear envelope disrupts the Rb1/E2F and MyoD pathways during muscle regeneration. Hum. Mol. Genet. **15:**637–651.
30. **Muchir, A., P. Pavlidis, G. Bonne, Y. K. Hayashi, and H. J. Worman.** 2007. Activation of MAPK in hearts of EMD null mice: similarities between mouse models of X-linked and autosomal dominant Emery Dreifuss muscular dystrophy. Hum. Mol. Genet. **16:**1884–1895.
31. **Musaro, A., C. Giacinti, G. Borsellino, G. Dobrowolny, L. Pelosi, L. Cairns, S. Ottolenghi, G. Cossu, G. Bernardi, L. Battistini, M. Molinaro, and N. Rosenthal.** 2004. Stem cell-mediated muscle regeneration is enhanced by local isoform of insulin-like growth factor 1. Proc. Natl. Acad. Sci. USA **101:**1206–1210.
32. **Musaro, A., K. McCullagh, A. Paul, L. Houghton, G. Dobrowolny, M. Molinaro, E. R. Barton, H. L. Sweeney, and N. Rosenthal.** 2001. Localized Igf-1 transgene expression sustains hypertrophy and regeneration in senescent skeletal muscle. Nat. Genet. **27:**195–200.
33. **Naya, F. J., and E. Olson.** 1999. MEF2: a transcriptional target for signaling pathways controlling skeletal muscle growth and differentiation. Curr. Opin. Cell Biol. **11:**683–688.
34. **Olson, E. N.** 1992. Interplay between proliferation and differentiation within the myogenic lineage. Dev. Biol. **154:**261–272.
35. **Park, I. H., E. Erbay, P. Nuzzi, and J. Chen.** 2005. Skeletal myocyte hypertrophy requires mTOR kinase activity and S6K1. Exp. Cell Res. **309:**211–219.
36. **Ren, H., P. Yin, and C. Duan.** 2008. IGFBP-5 regulates muscle cell differentiation by binding to IGF-II and switching on the IGF-II auto-regulation loop. J. Cell Biol. **182:**979–991.
37. **Rommel, C., S. C. Bodine, B. A. Clarke, R. Rossman, L. Nunez, T. N. Stitt, G. D. Yancopoulos, and D. J. Glass.** 2001. Mediation of IGF-1-induced skeletal myotube hypertrophy by PI(3)K/Akt/mTOR and PI(3)K/Akt/GSK3 pathways. Nat. Cell Biol. **3:**1009–1013.
38. **Schirmer, E. C., L. Florens, T. Guan, J. R. Yates III, and L. Gerace.** 2003. Nuclear membrane proteins with potential disease links found by subtractive proteomics. Science **301:**1380–1382.
39. **Shiraishi, S., C. Zhou, T. Aoki, N. Sato, T. Chiba, K. Tanaka, S. Yoshida, Y. Nabeshima, Y. Nabeshima, and T. A. Tamura.** 2007. TBP-interacting protein

120B (TIP120B)/cullin-associated and neddylation-dissociated 2 (CAND2) inhibits SCF-dependent ubiquitination of myogenin and accelerates myogenic differentiation. J. Biol. Chem. **282:**9017–9028.
40. **Sigal, Y. J., M. I. McDermott, and A. J. Morris.** 2005. Integral membrane lipid phosphatases/phosphotransferases: common structure and diverse functions. Biochem. J. **387:**281–293.
41. **Simon, A. J.** 2007. Nuclear lamina organization and new functions. The wall and yard guardians of gene expression. FEBS J. **274:**1353.
42. **Tabb, D. L., W. H. McDonald, and J. R. Yates III.** 2002. DTASelect and Contrast: tools for assembling and comparing protein identifications from shotgun proteomics. J. Proteome Res. **1:**21–26.
43. **Takeuchi, M., M. Harigai, S. Momohara, E. Ball, J. Abe, K. Furuichi, and N. Kamatani.** 2007. Cloning and characterization of DPPL1 and DPPL2, representatives of a novel type of mammalian phosphatidate phosphatase. Gene **399:**174–180.
44. **Tollefsen, S. E., J. L. Sadow, and P. Rotwein.** 1989. Coordinate expression of insulin-like growth factor II and its receptor during muscle differentiation. Proc. Natl. Acad. Sci. USA **86:**1543–1547.
45. **Vander, H. E., S. I. Lee, S. Bandhakavi, T. J. Griffin, and D. H. Kim.** 2007. Insulin signalling to mTOR mediated by the Akt/PKB substrate PRAS40. Nat. Cell Biol. **9:**316–323.
46. **Washburn, M. P., D. Wolters, and J. R. Yates III.** 2001. Large-scale analysis of the yeast proteome by multidimensional protein identification technology. Nat. Biotechnol. **19:**242–247.
47. **Weintraub, H.** 1993. The MyoD family and myogenesis: redundancy, networks, and thresholds. Cell **75:**1241–1244.
48. **Wolters, D. A., M. P. Washburn, and J. R. Yates III.** 2001. An automated multidimensional protein identification technology for shotgun proteomics. Anal. Chem. **73:**5683–5690.
49. **Wu, A. L., J. H. Kim, C. Zhang, T. G. Unterman, and J. Chen.** 2008. Forkhead box protein O1 negatively regulates skeletal myocyte differentiation through degradation of mammalian target of rapamycin pathway components. Endocrinology **149:**1407–1414.
50. **Yoon, M. S., and J. Chen.** 2008. PLD regulates myoblast differentiation through the mTOR-IGF2 pathway. J. Cell Sci. **121:**282–289.
51. **Zhang, X., L. Shu, H. Hosoi, K. G. Murti, and P. J. Houghton.** 2002. Predominant nuclear localization of mammalian target of rapamycin in normal and malignant cells in culture. J. Biol. Chem. **277:**28127–28134.